SIAM J. Applied Dynamical Systems
Vol. 0, No. 0, pp. 000–000

Long Period Oscillations in a G_0 Model of Hematopoietic Stem Cells*

Laurent Pujo-Menjouet†, Samuel Bernard‡, and Michael C. Mackey§

Abstract. This paper analyzes the dynamics of a G_0 cell cycle model of pluripotential stem cells so we can understand the origin of the long period oscillations of blood cell levels observed in periodic chronic myelogenous leukemia (PCML). The model dynamics are described by a system of two delayed differential equations. We give conditions for the local stability of the nontrivial steady state. We use these conditions to study when stability is lost and oscillations occur, and how various parameters modify the period of these oscillations. We consider a limiting case of the original model in order to compute an explicit solution and give an exact form of the period and the amplitude of oscillations. We illustrate these results numerically and show that the main parameters controlling the period are the cellular loss (the differentiation rate δ and the apoptosis rate γ), while the cell regulation parameters (proliferation rate β and cell cycle duration τ) mainly influence the amplitude.

Key words. cell proliferation, G_0 stem cell model, periodic chronic myelogenous leukemia, long period oscillations, delay differential equations, Hill function

AMS subject classifications. 34C25, 34K18, 37G15

DOI. 10.1137/030600473

1. Introduction.

Hematological diseases have attracted a significant amount of modeling attention [1, 22, 18, 17, 19, 20, 21, 33, 41, 44, 45, 47, 56, 58]. This is primarily because of the existence of periodic hematological diseases, in which there are clear and statistically significant oscillations in the number of circulating cells with periods ranging from weeks to months [30].

Some of these periodic hematological diseases involve only one type of blood cell, and all of these seem to be due to a destabilization of a peripheral control mechanism, e.g., periodic auto-immune hemolytic anemia [5, 46] and cyclical thrombocytopenia [59, 62]. It is commonly observed that periodic hematological diseases of this type involve periodicities between two and four times the bone marrow production delay, and this observation has a clear explanation within a modeling context.

Other periodic hematological diseases show oscillations in all of the circulating blood cells (i.e., white cells, red blood cells, and platelets). These diseases often have periods that are

*Received by the editors July 16, 2003; accepted for publication (in revised form) by B. Ermentrout September 15, 2004; published electronically DATE.
http://www.siam.org/journals/siads/x-x/60047.html

†Department of Physiology, Physics and Mathematics, Centre for Nonlinear Dynamics, McGill University, 3655 Drummond Street, Montreal, Quebec, Canada H3G 1Y6 (pujo@cnd.mcgill.ca). The work of this author was supported by MITACS (Canada).

‡Current address: Institute for Theoretical Biology, Humboldt University (s.bernard@biologie.hu-berlin.de). The work of this author was supported by MITACS (Canada) and ISM (Québec).

§Departments of Physiology, Centre for Nonlinear Dynamics, McGill University, 3655 Drummond, Montréal, Québec H3G 1Y6 CANADA (mackey@cnd.mcgill.ca). The work of this author was supported by the Natural Sciences and Engineering Research Council (NSERC grant OGP-0036920, Canada), MITACS (Canada), and Le Fonds pour la Formation de Chercheurs et l'Aide à la Recherche (FCAR grant 98ER1057, Québec).

quite long (on the order of weeks to months) and are believed to be due to a destabilization of the pluripotential stem cell population from which all of the mature blood cell types are derived. This is observed in cyclical neutropenia [7, 8, 9, 30, 32, 44, 45, 47] and in chronic myelogenous leukemia (CML) [26]. This latter disease is the focus of the present paper.

Leukemia is a progressive, malignant disease of the blood-forming organs, characterized by uncontrolled proliferation of immature and abnormal white blood cells in the bone marrow, the blood, the spleen, and the liver. It is classified clinically on the basis of the character of the disease (chronic or acute), the type of cells involved (myeloid, lymphoid, or monocytic), and the increase or lack of increase in the number of abnormal cells in the blood (leukemic or aleukemic). In this paper we focus our attention on CML and more specifically on its periodic form.

CML is characterized by a chromosomal translocation. Typically, leukemic cells share a chromosome abnormality not found in nonleukemic white blood cells or in other cells of the body. This abnormality is a reciprocal translocation between chromosome 9 and chromosome 22. This translocation results in chromosome 9 being longer than normal and chromosome 22 being shorter than normal. The DNA removed from chromosome 9 contains most of the proto-oncogene designated c-Abl, and the break in chromosome 22 located in the middle of the gene is designated by Bcr. The resulting *Philadelphia chromosome* has the section of Bcr fused with most of c-Abl. We then have a chimeric protein Brc-Abl tyrosine kinase (PTK) that causes a leukemia-like disease [16, 24, 28, 36, 39, 42, 43, 66].

CML is believed to arise in the hematopoietic stem cell compartment based in the bone marrow that supplies progeny for all of the cellular elements of the blood. Two main lines of evidence support this belief. First, in CML patients it is generally observed that the Philadelphia chromosome can be found in all of the hematopoietic lineages [12, 23, 29, 35, 63] implying that these cells are all derived from a common ancestor containing the Philadelphia chromosome. The second line of evidence is based on observations in patients with the variant periodic CML (PCML). In this relatively rare form of the disease, white blood cells, platelets, and erythrocyte precursors all oscillate with the same period [26] (see Figure 1.1). The most parsimonious explanation is that this oscillation is derivative from a central oscillation in the efflux of primitive committed cells from the pluripotential stem cell population.

It has long been known that there is a large variation between patients in the length of the period of the oscillations in PCML (between 40 to 80 days) [26]. Even more puzzling is the fact that there is an enormous difference between the periods involved in PCML and the average pluripotential cell cycle duration which ranges between one to four days [38, 47, 48]. The connection between the relatively short cell cycle durations and the relatively long periods of peripheral cell oscillations is unclear and not understood. The most important question is then, "How do *short* cell cycles give rise to *long* period oscillations?"

To understand the dynamics of PCML, we consider a model for the regulation of stem cell dynamics. We employ a G_0 model for the stem cell population, whose early features are due to Lajtha [40] and Burns and Tannock [14]. We wish to understand the influence of parameters in this stem cell model on the oscillation period when the model becomes unstable and starts to oscillate.

This paper is organized as follows. In section 2, we describe the stem cell model in detail and present an existence and uniqueness result for the solutions of the model equation. In

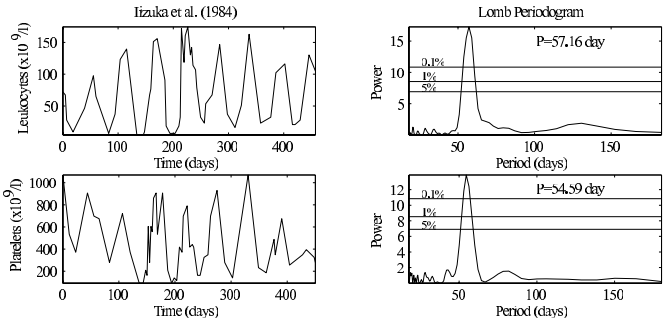

Figure 1.1. *Published data and analysis of leukocyte, platelet, and reticulocyte population for one PCML patient* [34]. *The left column contains the serial blood counts, and the right column contains the corresponding Lomb periodogram P(T) (power P versus period T in days). The dashed line in the left column represents the normal level of cells, and the horizontal lines in the Lomb periodogram give the* $p = 0.05$, $p = 0.01$, *and* $p = 0.001$ *significance levels. The details of the computations of the Lomb periodogram can be found in* [26].

section 3, we study the nontrivial steady state of the system and its local stability. Section 4 considers the case where the solutions are periodic. We introduce a method of deriving the solution analytically and give an explicit form for the period and amplitude of the solutions. We then give some numerical illustrations of this result as parameters are varied. In section 5, we give a short conclusion.

2. Description of the stem cell model.

The stem cell model that we consider is a classical G_0 model [14, 50, 61] that partitions cells, based on their functional status, into one of two phases: a proliferating phrase and a resting phase (the so-called G_0-phase). The proliferating cell population consists of those cells actively engaged in the synthesis of DNA and ultimately undergoing mitosis and cytokinesis. The numbers of proliferating phase cells are denoted by $P(t)$, where t is time. In this proliferating phase, cells are committed to undergo cell division a constant time τ after entry or be lost through apoptosis at a constant rate γ. At the point of cytokinesis, a cell divides into two daughter cells which enter the resting phase (see Figure 2.1). The resting phase (G_0) cells are denoted by $N(t)$. Cells in the resting phase, by definition, cannot divide. They may have one of three possible fates. They may differentiate at a constant rate δ, they may reenter the proliferating phase at a rate β, or they may simply remain in G_0.

The full model for this situation consists of a pair of (age-structured) reaction convection evolution equations with their associated boundary and initial conditions [58, 44, 45, 51]. Using the method of characteristics [65], these equations can be transformed into a pair of nonlinear first-order differential delay equations [44, 45, 47]:

$$\frac{dP(t)}{dt} = -\gamma P(t) + \beta(N)N - e^{-\gamma\tau}\beta(N_\tau)N_\tau, \tag{2.1}$$

$$\frac{dN(t)}{dt} = -[\beta(N) + \delta]N + 2e^{-\gamma\tau}\beta(N_\tau)N_\tau, \tag{2.2}$$

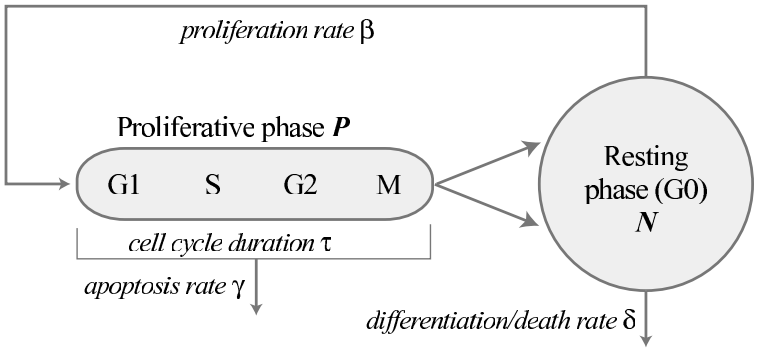

Figure 2.1. *A schematic representation of the G_0 stem cell model. Proliferating phase cells (P) include those cells in G_1, S (DNA synthesis), G_2, and M (mitosis), while the resting phase (N) cells are in the G_0-phase. δ is the rate of differentiation into all the committed stem cell populations, and γ represents a loss of proliferating phase cells due to apoptosis. β is the rate of cell reentry from G_0 into the proliferative phase, and τ is the duration of the proliferative phase. See [44, 45, 47] for further details.*

where $N_\tau \equiv N(t-\tau)$. The term $e^{-\gamma\tau}\beta(N_\tau)N_\tau$ in (2.1) represents the number of surviving cells leaving the proliferating phase that entered a time $t-\tau$ earlier. The term $2e^{-\gamma\tau}\beta(N_\tau)N_\tau$ in (2.2) represents the newly born daughter cells coming from the surviving mother cells.

The resting-to-proliferative phase feedback rate β (i.e., the mitotic reentry rate from G_0 into proliferation) is taken to be a monotone decreasing Hill function of N

$$\beta(N) = \beta_0 \frac{\theta^n}{\theta^n + N^n}. \tag{2.3}$$

In (2.3), β_0 is the maximal rate of cell movement from G_0 into proliferation, θ is the G_0 stem cell population at which the rate of cell movement from G_0 into proliferation is one-half of its maximal value (β_0), and $n > 0$ characterizes the sensitivity of the mitotic reentry rate β to changes in the size of G_0. The Hill function $\beta(N)$ has often been used in cell cycle models to describe saturation (see [25], for instance). The choice of this form for β is standard and can be found in [13, 54, 44].

Note that the dynamics of the resting phase cells described by (2.2) are independent of the dynamics of the proliferative phase cells but the converse is not true. This is due to the assumed dependence of β on N as well as the boundary conditions of the original equations of the problem [44, 45]. Because of this independence, we need only concern ourselves with (2.2) in the rest of the paper. A solution of (2.2) is a continuous function $N : [-\tau, +\infty) \to \mathbb{R}_+$ obeying (2.2) for all $t > 0$. The continuous function $\varphi : [-\tau, 0) \to \mathbb{R}_+$, $\varphi(t) = N(t)$ for all $t \in [-\tau, 0]$ is called the initial condition for N. Using the method of steps, it is easy to prove that for every $\varphi \in C([-\tau, 0])$, where $C([-\tau, 0])$ is the space of continuous functions on $[-\tau, 0]$, there is a unique solution of (2.2) (see, for instance, [51]).

3. Steady states and local stability. The objective of this paper is to understand the origin of stem cell related periodic hematological disease. Consequently, in this section we determine conditions such that the solutions of the nonlinear differential delay equation (2.2) are locally stable. In particular, we investigate the regions of parameter space where the

solutions become unstable through a Hopf bifurcation.

3.1. Steady states. The steady states N_* of (2.2) are given by the solutions of $dN/dt \equiv 0$. It is clear that they must satisfy either $N_* \equiv 0$ (the trivial steady state) or

$$N_* = \theta \left(\frac{\beta_0}{\delta}(2e^{-\gamma\tau} - 1) - 1 \right)^{1/n} = \theta \left(\frac{\beta_0}{\beta_*} - 1 \right)^{1/n}.$$

For the positive steady state to exist it is necessary for the following conditions to be satisfied:

$$0 \le \tau \le \tau_{max} \equiv -\frac{1}{\gamma} \ln \left[\frac{\delta + \beta_0}{2\beta_0} \right] \text{ and } \delta < \beta_0. \tag{3.1}$$

In the rest of the paper we consider τ in the interval $[0, \tau_{max}]$. The trivial steady state $N_* \equiv 0$ corresponds to the death of the population. Consequently, we focus our attention on the nontrivial steady state. It will be shown, however, that the stability of the trivial steady state is relevant for proving the existence of the periodic solutions in section 4.1.

3.2. Local stability. Define a dimensionless variable $x = N/\theta$ so we can write the dynamical equation for the nonproliferating population of cells as

$$\frac{dx}{dt} = -\left[\beta(x) + \delta\right] x + \kappa\beta(x_\tau)x_\tau, \tag{3.2}$$

where $\kappa(\tau) = 2e^{-\gamma\tau}$ and $\beta_* = \frac{\delta}{\kappa - 1}$. To examine the local stability of the steady state

$$x_* = \left(\frac{\beta_0}{\beta_*} - 1 \right)^{1/n},$$

we linearize (3.2) in the neighborhood of x_*. Denote the deviation of x away from the steady state value by $z = x - x_*$, and set $B^\tau = \beta_* + \beta'_* x_*$ to obtain

$$\frac{dz}{dt} = -\left[B + \delta\right] z + \kappa B z_\tau. \tag{3.3}$$

(The notation B^τ is used to indicate the implicit dependence of B on τ through the parameter κ.)

If we make the ansatz that $z(t) \sim e^{\lambda t}$ in (3.3), then the eigenvalue equation $\lambda + (\delta + B) = \kappa B e^{-\lambda\tau}$ results immediately. This transcendental equation has been studied by Hayes [31] and Beretta and Kuang [6] who have derived necessary and sufficient conditions for $\Re(\lambda) \le 0$, which corresponds to a locally stable steady state x_*.

In our situation, these conditions depend on the value of n, and we consider two cases: $n \in [0, 1]$ and $n > 1$. For $n \in [0, 1]$, the solutions are locally stable for $\tau \in [0, \tau_{max}]$. For $n > 1$, two subcases must be considered:

1. If $n\delta \ge (n-1)\beta_0$, the solutions are locally stable for $\tau \in [0, \tau_{max}]$.
2. If $0 \le n\delta < (n-1)\beta_0$, define

$$\tau_n = -\frac{1}{\gamma} \ln \left\{ \frac{1}{2} \left[\frac{\delta}{\beta_0} \left(1 + \frac{1}{n-1} \right) + 1 \right] \right\}.$$

(a) For $\tau \in [0, \tau_n]$, note that $B \leq 0$. We then have stability if and only if $-1 \leq \frac{\kappa B}{\delta + B} \leq 1$, or

$$-1 \leq \frac{\delta + B}{\kappa B} \leq 1 \quad \text{and} \quad \tau < \tau_{crit} \equiv \frac{\cos^{-1}\left(\frac{\delta + B}{\kappa B}\right)}{\sqrt{(\kappa B)^2 - (\delta + B)^2}}.$$

(b) For $\tau \in [\tau_n, \tau_{max}]$ the solutions are locally stable.

The details of the computations leading to these results are in Appendix A. Note that these inequalities are implicit and involve four different parameters. It is the goal of this paper to understand the role of each in determining the characteristics of periodic solutions to the stem cell model.

Since it is only for case 2a that periodic solutions may arise, we now focus our attention there. Note that $\lambda = 0$ is not a root of the eigenvalue equation. It is then clear that if the equilibrium loses its stability, this must occur through a Hopf bifurcation. In other words, if the parameters B, δ, κ are such that $\tau \equiv \tau_{crit}$, then there is a Hopf bifurcation with pure imaginary eigenvalues $\lambda = \pm i\omega$, ω being a positive real number, and there is a periodic solution of (3.3) with *Hopf period* $T_H = 2\pi/\omega$ given by

$$T_H = \frac{2\pi}{\sqrt{(\kappa B)^2 - (\delta + B)^2}} = \frac{2\pi\tau_{crit}}{\cos^{-1}\left(\frac{\delta + B}{\kappa B}\right)}. \tag{3.4}$$

These results clearly show when we might expect to find long period oscillatory behavior in (2.2)—namely, when $\tau > \tau_{crit}$ and $\gamma\tau \to \ln 2$ or, equivalently, $\kappa \to 1$. However, long period oscillations do not necessarily have large amplitudes as we shall see in the numerical results presented in section 4. It is thus important to understand the link between the period and the amplitude of the oscillation to make the connection between model behavior and clinical data as strong as possible. Due to the complexity of the equations, we are unable to delineate these conditions analytically but have determined then numerically in sections 3.3 and 4.2.

3.3. Long period solutions. In this short section, we numerically illustrate some of the analytic results obtained in section 3.2.

One of the authors [44, 47, 48] has estimated standard values of the parameters in our model as shown in Table 3.1. In our numerical simulations we will use this set as a basis for all investigations of parameter changes. Thus, when the effect of changing one or more parameters is being investigated, all of the other parameters will be held at the values in Table 3.1.

The results presented in Figure 3.1 show the influence of the Hill coefficient n on the solutions of (3.2). For these parameters, the steady state $x_* \simeq 21.57^{1/n}$, and it is obvious that the steady state decreases when n increases. When $n \geq 10$ oscillations appear around the steady state (see Figure 3.1(A)). The larger the Hill coefficient n, the larger the period and amplitude of the oscillation (see Figure 3.1(B)). However, because the Hill function β is an asymptotically decreasing function that approaches a Heaviside function as n tends to

Table 3.1
Standard parameters for the cell cycle model.

Parameter	Value
δ	0.05 day^{-1}
τ	1 day
β_0	1.77 day^{-1}
γ	0.2 day^{-1}

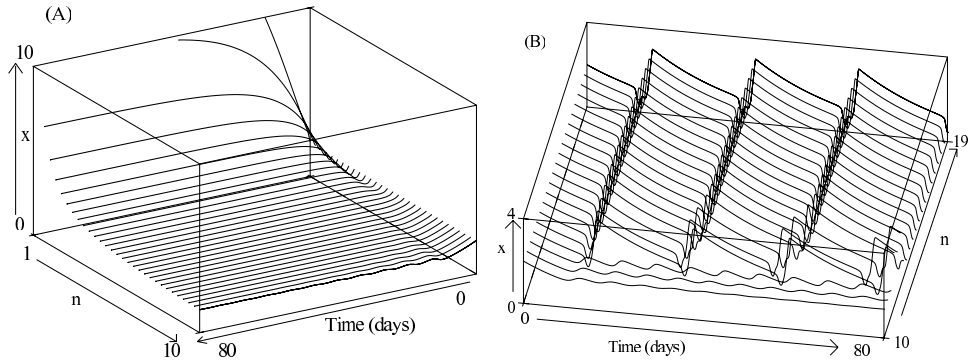

Figure 3.1. (A) *Ultrasensitive response of the solution of* (3.2) *with Hill coefficients n from* 1 *to* 10*, with all other parameters taken from Table* 3.1. (B) *Ultrasensitive response of the solution of* (3.2) *with Hill coefficients n from* 10 *to* 19*, with all other parameters taken from Table* 3.1.

infinity maximum amplitude A and period T as $n \to \infty$, it is then necessary to change other parameters to modify A and T.

In [57] the authors numerically investigated the influence of each parameter (τ, δ, γ, β_0, and n) on the oscillation characteristics. Although the study presented in [57] is a rather complete review of the different period lengths a solution can show under changes of the parameters, they were unable to obtain any accurate results on the slight changes of amplitude occurring with these parameter changes.

The goal of the next section is to develop a technique to obtain an implicit analytic expression for the amplitude when n tends to infinity. Even though the analytic result is only implicit, it allows us to carry out a quite accurate numerical study.

4. Approximation of the long period solutions. In this section we analytically study the periodic solution properties of (3.2). Since β given by (2.3) is a decreasing function, our model corresponds to a (nonlinear) negative feedback loop with delay. Few general techniques are available to predict the behavior of such systems, and one has often to rely on numerical simulations. However, there is a class of delay differential equations that is amenable to analytic treatment (c.f. [3, 4, 49, 55, 64] and the more recent papers [1, 51, 52]). In this section we use these techniques, as applied by Mackey and an der Heiden [49], for a limiting form of the function β.

Consider the Hill function given by (2.3) that defines β. If the Hill coefficient $n \to \infty$, then β becomes a piecewise constant function (a Heaviside step function), and a complete characterization of the solutions is possible. Moreover, we can see in Figure 3.1(A) that

considering $n \simeq 12$ is already a good approximation of a high Hill coefficient for our numerical simulations. The Hill coefficient is often regarded as a cooperativity coefficient, describing the number of agents (molecules, proteins, or complexes) required to activate or deactivate a given process. If n was interpreted to be the number of ligand molecules required to activate or deactivate a receptor site, then values of $n = 12$ or larger would not be biologically realistic. However, there are other situations in which cascade effects are known to create switch-like phenomena [25]. In these circumstances, both experimental data and theoretical modeling suggest that the large values of n considered are quite realistic [11, 10].

4.1. Reduction of the model for large n. When $n \to \infty$, the feedback function β can be approximated by the Heaviside step function

$$\beta(x_\tau) = \beta_0 \left[1 - H(x_\tau - \theta)\right], \tag{4.1}$$

where

$$H(y) = \begin{cases} 1 & \text{if} \quad y \geq 0, \\ 0 & \text{otherwise.} \end{cases} \tag{4.2}$$

From now on we take $\theta = 1$. If we define two new constants by

$$\alpha = \beta_0 + \delta \ \text{ and } \ \Gamma = 2\beta_0 e^{-\gamma\tau} = \kappa\beta_0, \tag{4.3}$$

then the full model dynamics are given by

$$\frac{dx}{dt} = \begin{cases} -\delta x & \text{for } \ 1 \leq x, x_\tau, \\ -\alpha x & \text{for } \ 0 \leq x < 1 \leq x_\tau, \\ -\alpha x + \Gamma x_\tau & \text{for } \ 0 \leq x, x_\tau < 1, \\ -\delta x + \Gamma x_\tau & \text{for } \ 0 \leq x_\tau < 1 \leq x. \end{cases} \tag{4.4}$$

This new equation allows us to state our main result. The utility of this result is a consequence of the method of proof which is given in Appendix B.

Consider a fixed positive constant τ. From the last two equations of (4.4) it is obvious (see Appendix B for the argument) that the parameter Γ has to be large enough for the solution to oscillate. If this is not the case, the solution will decrease to 0 as t approaches infinity. It is sufficient then to impose the condition

$$\Gamma > \alpha e^{-\alpha\tau} \tag{4.5}$$

so that $\Gamma x_\tau > \alpha x$. A detailed computation leading to the condition (4.5) can be found in Appendix B. One of the main arguments for choosing this condition is the following. If we consider the initial function $\varphi(t) > 1$ for $t \in [-\tau, 0]$, then the solution decreases to a minimum value $\alpha e^{-\alpha\tau}$ after a certain time $t_1 + \tau$, where $x(t_1) = 1$. Then if condition (4.5) is satisfied, the solution will increase after the time $t_1 + \tau$ to a maximum value that would be hopefully required to be higher than 1. To get this maximum value higher than 1 we have to add some other conditions on Γ. Using some simple computations, it is possible to show that if

$$\Gamma > \max\{\alpha e^{-\alpha\tau}, (e^{\alpha\tau} - e^{-\alpha\tau})/\tau\}, \tag{4.6}$$

then the solution of (4.4) will reach its maximum above the critical value 1 for a time $t \in [t_1+\tau, t_1+2\tau]$. This condition will force the slope of the increasing portion of the solution to be steep, and the period will be short. It is actually possible to give some other conditions on Γ so that the maximum value could be reached after the time $t_1+2\tau$. Thus the period would be longer. However, in our main result presented below, we want to prove that the solution is periodic and can get long oscillation periods. Consequently, we give conditions to obtain periodic solutions having a minimum period. By a simple computation, it is then possible to deduce from this result the conditions to get the period as long as one wish. This is why, as we shall see further in the numerical illustration, it is possible to choose ad hoc parameters to obtain longer periods. Note that if we consider the initial function φ such that $\varphi(t) < 1$ for $t \in [-\tau, 0]$, the techniques are the same and so is the result, except that we need $\Gamma > \alpha$ instead of condition (4.5). For simplicity, in the following result, we consider only the case where $\varphi(t) > 1$ for $t \in [-\tau, 0]$ and condition (4.6) to get the shortest period oscillation. The other cases can be deduced using the same techniques.

Proposition 4.1. *Assume that $x(t)$ is solution of (4.4) with an initial condition $\varphi \in C([-\tau, 0])$, where φ is such that*

$$\varphi(t) > 1 \quad \textit{for } t \in [-\tau, 0]\,. \tag{4.7}$$

Suppose also that Γ satisfies (4.6). Then $x(t)$ is an orbitally stable periodic solution with a period larger than 2τ.

From a biological point of view, condition $\Gamma > \alpha e^{-\alpha\tau}$ means that the maximum number of new daughter cells entering the resting phase is larger than the number of cells leaving it (by differentiation, death, or reintroduction into the proliferating cells). The condition $\Gamma > (e^{\alpha\tau} - e^{-\alpha\tau})/\tau$ is more technical and does not have any obvious biological interpretation.

Proof. The detailed proof is given in Appendix B. However, for clarity, we give a brief outline of the thread of the proof to highlight the main steps (cf. Figure 4.1). From the value of the initial function, and by continuity of the solution, we solve (4.4) for x and x_τ larger than 1, which corresponds to the first differential equation of this system. The solution is decreasing up to a time t_1 such that $x(t_1) = 1$. Then $x < 1$ while x_τ is still larger than 1. So, we solve the solution of the second differential equation of the system (4.4). The function decreases until a time $t_1+\tau$ where both x and x_τ are less than 1. In order to obtain a periodic solution we apply condition (4.6) so that the solution increases again as a solution of the third differential of the system. Otherwise, the populations tends to zero as t goes to infinity. Under condition (4.6) the solution increases up to a time $t_2 < t_1 + 2\tau$, where it again crosses the line $y = 1$. Consequently, it is possible to show that after a certain time at least equal to 2τ the solution comes back to its original value. This, in turn, allows us to give the period explicitly. ■

4.2. Numerical illustration of the results. We present some numerical results for the solutions of (4.4) corresponding to $n \to \infty$, made using MATLAB with the delay differential equation solver `dde23` [60]. The results of our investigations are shown in Figures 4.2 through 4.6.

These simulations have three main objectives.

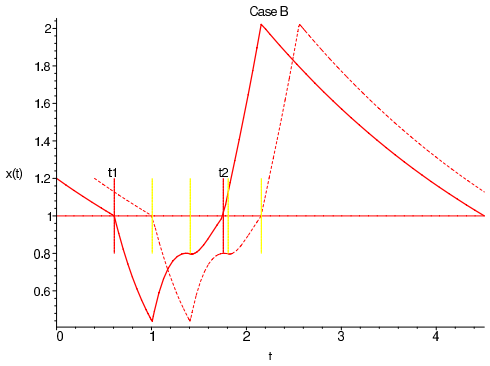

Figure 4.1. *Sketch of the solution related to the case B of the proof given in the Appendix B.*

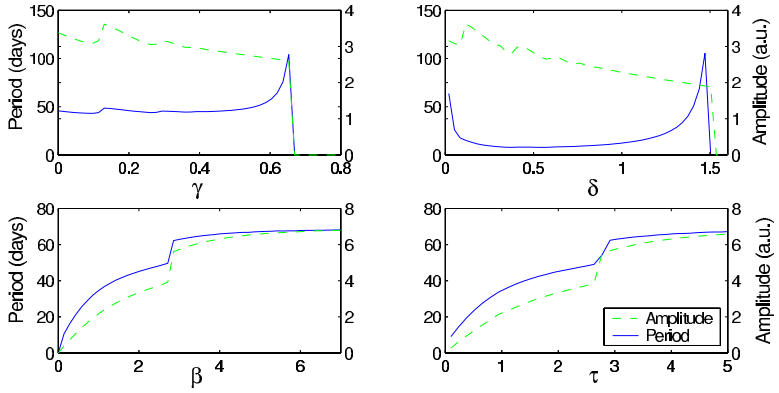

Figure 4.2. *Evolution of period and amplitude of the solutions of (4.4) when $n \to \infty$ and each of the four parameters is varied. In clockwise order from the top left the parameter varied is $\gamma = 0$ to 0.8 day^{-1}, $\delta = 0$ to 1.5 day^{-1}, $\beta_0 = 0$ to 7 day^{-1} and $\tau = 0$ to 5 days. The parameters not varied are held at their values given in Table 3.1.*

- The first is to show the individual influence of each of the four parameters (γ, δ, β_0, and τ) on the amplitude A and period T of the solutions of (4.4) in Figures 4.2 and 4.3.
- The second objective is to investigate the behavior of A and T with respect to changes in two parameters at a time as shown in Figure 4.4. The combinations are chosen in a specific way which is explained below.
- The third and last objective is to focus on the "ripples" in the solution behavior observed during the development of very long period oscillations.

4.2.1. Influence of each parameter individually. In Figure 4.2 we present the dependence of A and T on each of the parameters γ, δ, β_0, and τ, and the solutions themselves are illustrated in Figure 4.3. In Figure 4.3, the temporal solutions are plotted as a function of each of the four parameters γ, δ, β_0, and τ. In each panel, one can observe the different profiles taken by the solution, the evolution of the period T given by the shape of the ripples, and the evolution of the amplitude A given by the color coding (red for the highest amplitudes and blue for the lowest). This figure contains the results on which Figure 4.2 is based but

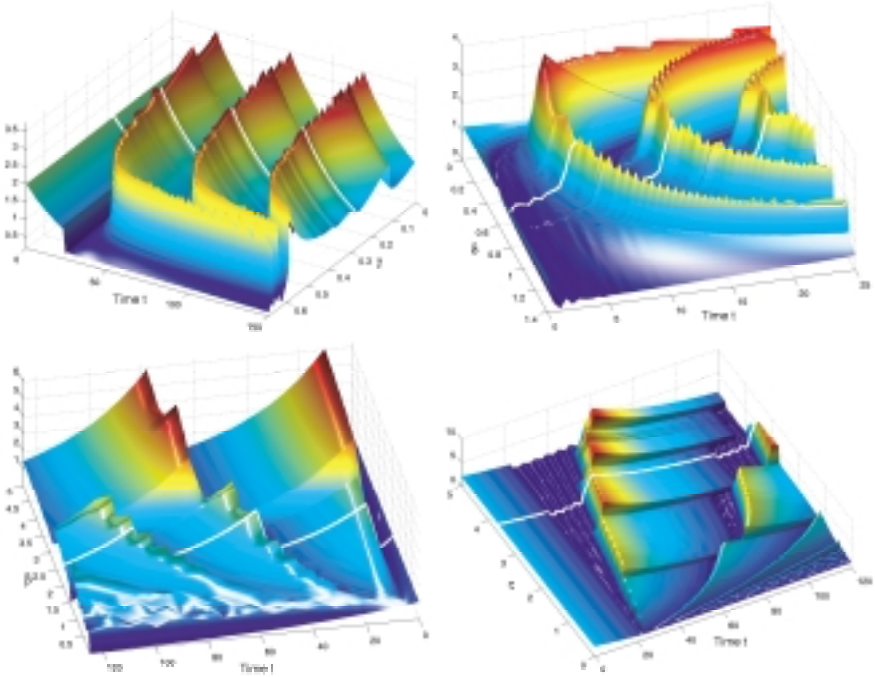

Figure 4.3. *Solution profiles of (4.4) when $n \to \infty$ and each of the four parameters is varied individually. In clockwise order from the top left the parameter varied is $\gamma = 0$ to 0.7 day^{-1}, $\delta = 0$ to 1.4 day^{-1}, $\tau = 0$ to 5 days, and $\beta_0 = 0$ to 5 day^{-1}. In each figure one can observe the solution behavior when a parameter changes, the evolution of the period, and the evolution of the amplitude through the color coding. The parameters that do not change on a figure are drawn from the parameter set in Table 3.1. The white line in each figure represents the solution for this fixed parameter set.*

offers more insight into solution dependencies on parameter changes. Indeed, by examining the solution profiles one can observe the formation of "ripples" before large transitions in period and/or amplitude which was impossible to illustrate in Figure 4.2. We will come back to these ripples later.

4.2.2. The effect of changing two parameters at the same time. From these results, two natural parameter groupings emerge.

1. The first one consists of γ and δ (the apoptosis and differentiation rates). As each one increases, there is generally a slight decrease in amplitude A, while period T can vary dramatically and increase to approach infinity. A and T are not simply correlated for this pair of parameters.

2. The second group consists of β_0 and τ. Increases in these two parameters give large increases in A but smaller increases in T than the first group. Note that changes in A and T are positively correlated with changes in β_0 and τ, so variations of β_0 or τ involve similar variations in both amplitude and period. The mechanism of this behavior is not well understood and is still under investigation.

Having identified these two parameter groupings, it is interesting to see how A and T depend on variation of two of the four parameters at the same time. We first choose to vary

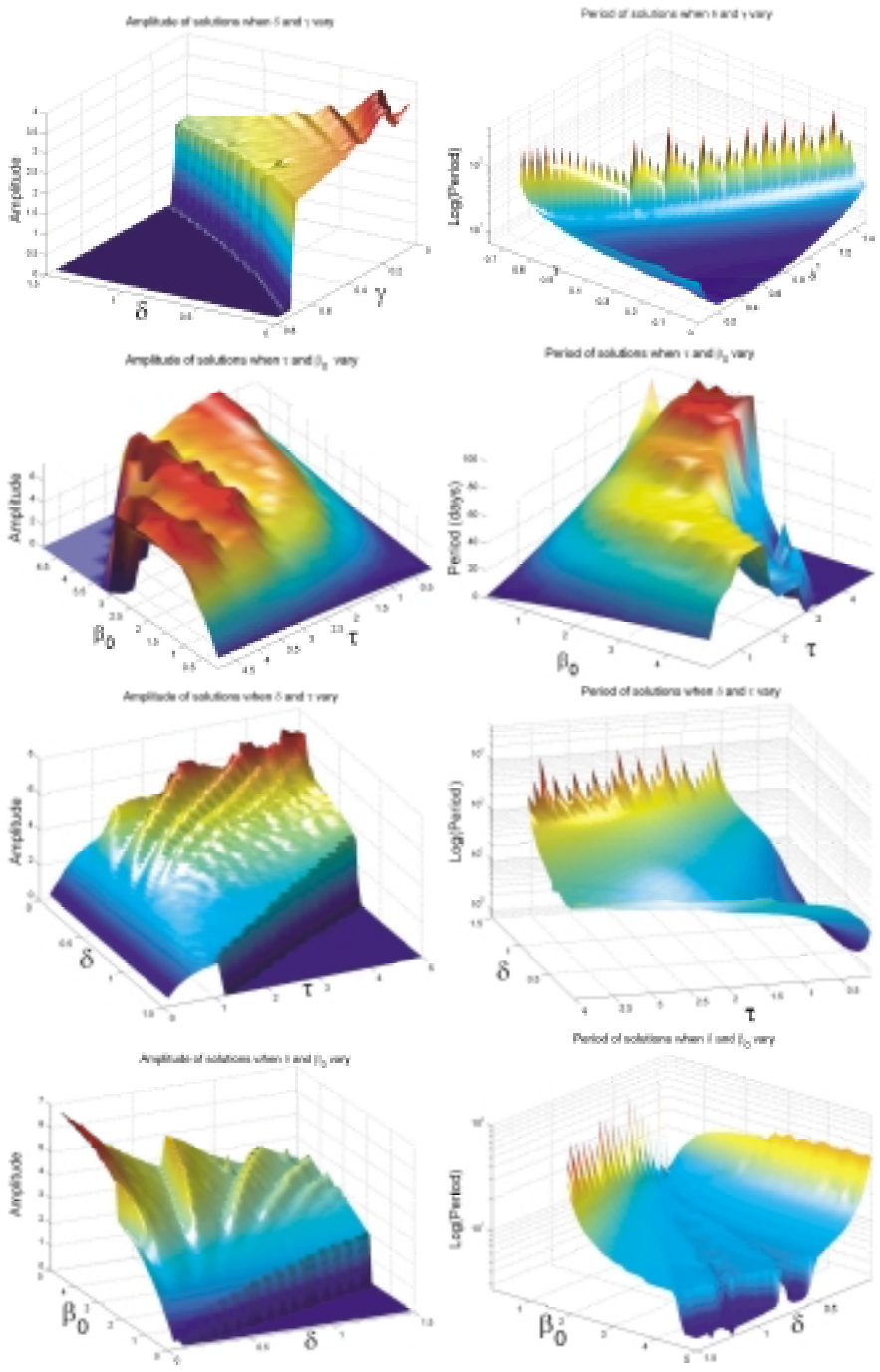

Figure 4.4. *Period and amplitude evolution when two parameters in* (4.4) *are varied at the same time. The amplitude is shown in the left-hand figures and the period in the right-hand figures. In the figures showing the periods, the sharply peaked lines represent the period approaching infinity. The parameters that do not change in a given figure are drawn from the parameter set of Table* 3.1.

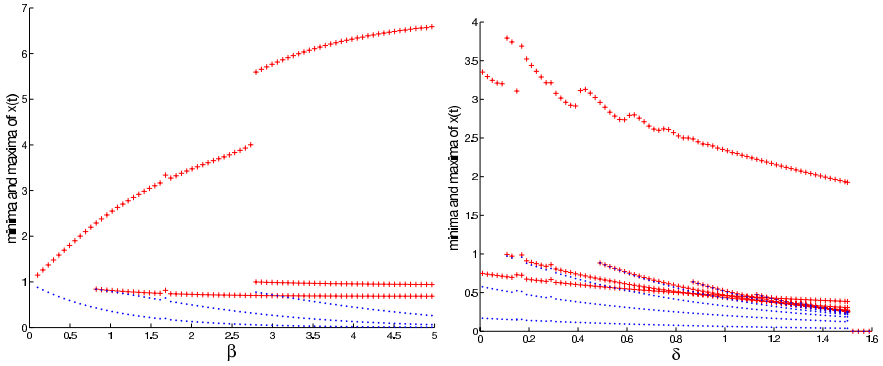

Figure 4.5. *Variation in the local maxima and minima with variations in β_0 and δ. The more local maxima and minima the solutions have, the longer the periods are, giving rise to the ripples observed in Figure 4.3 showing very long period oscillations. The parameters, when they do not vary, are taken from Table 3.1.*

parameters within the same group, i.e., δ and γ (the death and differentiation rates) and β_0 and τ (the cell cycle regulation parameters). Then we compare the effects of variation of one parameter from the death and differentiation group (we choose δ for our simulations, but the behavior is qualitatively the same with changes in γ) with changes in both of the cell cycle regulation parameters β_0 and τ. The results are presented in Figure 4.4 and can be summarized as follows.

For the death (γ) and differentiation (δ) rates, neither parameter has a predominant influence. Changes in both lead to slight changes of the same magnitude in A but can produce a dramatically long period T. For changes in the cell cycle regulation parameters β_0 and τ one also observes an approximately equal influence of both on both the amplitude A and period T. However, the influence of these on changes in the amplitude A is more profound than the effects of the death and differentiation rates.

When the amplitude is plotted as a function of the parameters β_0 and δ (Figure 4.4, bottom left) it is obvious that for small δ the influence of β_0 on A is greater than when δ is large.

4.2.3. Investigation of ripple formation. In this last section, we investigate the ripples observed when the period of the solution becomes very long. In Figure 4.5 we illustrate this for variations of β_0 and for δ. It is clear that each time a new wave appears it is accompanied by the appearance of another local minimum and local maximum. This number increases when the parameters increase (the number is larger when δ changes, corresponding to the fact that the influence of the death and differentiation rates have a larger influence on the period T than on the amplitude A).

Figure 4.6 examines how the local minima and maxima appear and change as τ is varied. As τ increases the number of ripples (cf. the three dimensional figure in the lower right portion of Figure 4.2). This is also shown on the upper right side where new local minima and maxima occur after $\tau = 1.2$, 2.6, 3.7, and 4.7. A plot of the solution $x(t)$ versus $x(t-\tau)$ (Figure 4.6(B)) shows that each time a new ripple appears it corresponds to a new small loop in the cycle. The appearance of each new loop is associated with an increase in the period T.

This pattern may be related to the onset of crises described in [15]. However, we observe

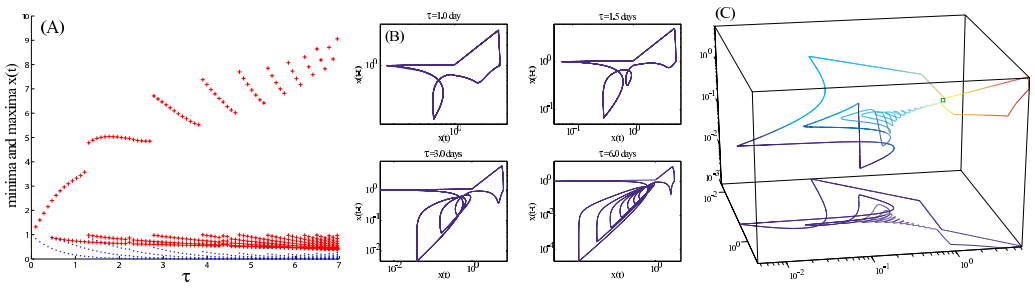

Figure 4.6. *Close-up of the case where τ varies. Observe that the local maxima and minima increase when τ increases* (A) *and the other parameters are taken from Table 3.1. On the projection of the solution onto the plane $x(t-\tau)$ versus $x(t)$, note that for each new local extremum a new loop appears* (B)*, where $\tau = 1, 1.5, 3,$ and 6, respectively. The behavior is, in fact, more complicated and can be plotted in three dimensions* (C)*, where $\tau = 3$ days and $\gamma = 0.18$ day^{-1}. This figure represents the solution in the $x(t-\tau)$ versus $x(t-\tau/2)$ versus $x(t)$ space. In the same figure we plot a projection of the solution on the plane $x(t-\tau/2)$ versus $x(t)$ to make a link with the qualitative behavior observed in graph* C.

neither period doubling nor subduction (i.e., the appearance of a nonchaotic attractor within a chaotic attractor causing the chaotic attractor to be replaced by the nonchaotic attractor involving the appearance of windows). This does not mean that it is impossible to find some cases where instability occurs with chaotic behaviors under certain conditions. Indeed, this has been proved analytically in [2] and [18]. This means that regarding our choice of parameters for which long period oscillations occur, the increase of the number of extrema does not occur by doubling but just through the successive adding of extrema without leading to chaos.

The increase of the period through the mechanism of increasing the number of extrema can be simply explained. Consider the case where the initial condition $\varphi(t)$ is such that $\varphi(t) > 1$ for $t \in [0, \tau]$ (see the computations of Appendix B). The solution of (4.4) decreases until a value t_1 such that $x(t_1) = 1$. Then the solution reaches a minimum value at time $t_1 + \tau$. If $\Gamma x_\tau > \alpha x$ (where Γ and α are defined by (4.3)), the solution increases after the time $t_1 + \tau$. To complete the period, the solution has to reach 1, which can be done for a value $t_2 > t_1$ such that $x(t_1) = 1$. However, if $\Gamma x_\tau \simeq \alpha x$, the slope of the curve is small, and it becomes very likely that after a time $t_{c1} \in [t_1 + \tau, t_2]$, $\Gamma x_\tau < \alpha x$, so that the curve decreases again until a time $t_{c2} > t_{c1}$ where $\Gamma x_\tau > \alpha x$, etc. Then, the solution increases slowly with many oscillations until the time t_2, after which $x(t) \geq 1$.

In Appendix B we analytically demonstrate the two first cases. Case A is one in which there is only one local minimum and one maximum and $t_2 \in [t_1 + \tau, t_1 + 2\tau]$. Case B corresponds to two local minima and maxima and $t_2 \in [t_1 + 2\tau, t_1 + 3\tau]$. These considerations can be extended indefinitely and the reader is welcome to compute the other tedious cases ($t_2 \in [t_1 + 3\tau, t_1 + 4\tau]$, etc.). These two cases show the mechanism of ripple production and how it is possible to obtain solutions with periods as long as wanted.

This phenomenon is, however, more complex, and a good way to show this complexity is to plot the solution in a three-dimensional space. When we plot the solution $x(t)$ versus $x(t-\tau)$ versus $x(t-\tau/2)$ to get the phase-three-dimensional figure (Figure 4.6(C)), one can see that 1 is an unstable point. The solution approaches 1 in an oscillatory fashion but is ultimately repulsed as it approaches 1, numerical evidence for the existence of a homoclinic

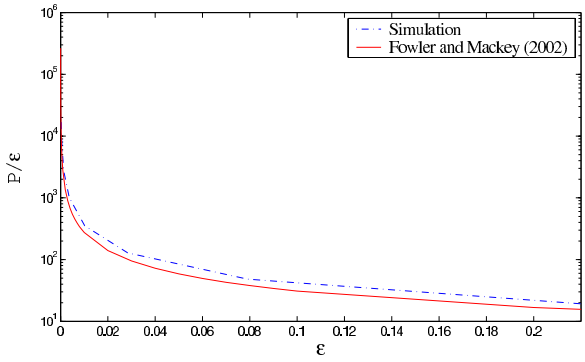

Figure 5.1. *Variation of the actual period P/ϵ as a function of ϵ (where $\epsilon = \delta\tau$ represents the rate of loss through differentiation), comparing the results obtained by Fowler and Mackey (Figure 4.2 of [27]) and in this paper. Because our approach is valid only for $n \to +\infty$, we take the same parameters as Fowler and Mackey, that is, $b = \beta_0\tau = 3.9$ and $\mu = (2e^{-\gamma\tau} - 1)/\tau = 1.2$, but we consider a larger value for n ($n = 20$ instead of 3).*

orbit. The analysis of this behavior is complicated and still under investigation.

5. Discussion and conclusions. Periodic chronic myelogenous leukemia (PCML) is a complex and poorly understood disease that is probably due to alterations at the stem cell level leading to oscillations in stem cell numbers and a consequent oscillation in cellular efflux, as well as other alterations in cellular maturation patterns. In this paper we have concentrated on the nature of the long period oscillations by analyzing the dynamics of a G_0 model for stem cell dynamics. This model contains four main parameters, and we have examined the role of each on the stem cell oscillation amplitude and period when the nontrivial steady state loses its stability.

The technique we have used is the same as used by Mackey and an der Heiden [49]. Although the examination of the solution behavior for $n \to \infty$ does not give information about the dynamics of the full problem, it does allow us to analytically investigate the role of each parameter in determining the period and the amplitude of the periodic solutions for the simplified problem.

Our results can be summarized as follows. We have shown that long period oscillations (period T on the order of weeks to months) in cellular efflux are possible even with short duration cell cycles τ (on the order of one to four days). We have also shown how the amplitude A and period T of these oscillations are determined by the four cell cycle parameters. Qualitatively, the cell cycle regulation parameters (β_0 and τ) have their major influence on the oscillation amplitude, while the oscillation period is correlated with the cell death and differentiation parameters (δ and γ). The importance of these four parameters has been recently shown by Moore and Lib in [53] for the case of CML. The authors use the latin hypercube sampling method, and they conclude that in CML the most promising research ways for treatments of this disease should be those that affect these specific parameters; this confirms our results.

In [27], Fowler and Mackey implement a new way of solving a nonlinear differential delay equation and, more particularly, the stem cell model we investigate here. This method is based

on the relaxation oscillation analysis of the Van der Pol oscillator developed by Kevorkian and Cole [37]. The authors have shown analytically that it is possible to obtain long period oscillations in the stem cell model when the proliferation rate is very small. Our approach is different but gives equivalent results. In Figure 5.1 we compare the period computed using our technique with the corresponding result given in Figure 4.2 of [27]. The same parameter values were used except for n which is taken to be $n = 20$ instead of $n = 3$ as used by Fowler and Mackey. (We use a large value of n because our results are only valid in this case.) The results corresponding to our two different approaches show the same quantitative results, illustrating the equivalence of the two different approaches.

Appendix A. Conditions for local stability. We assume that γ and τ are different from 0. Then, $\kappa(\tau) = 2e^{-\gamma\tau} > 0$ and $\beta_* = \delta/(\kappa - 1) > 0$. Before proving the stability results we note that $\kappa - 1 \neq 0$. Further, because of the definition of $x_* = (\beta_0/\beta_* - 1)^{1/n}$, we must have $\kappa - 1 > 0$, which is equivalent to $\tau < \ln 2/\gamma$. Moreover, from the definition of x_* we require

$$\beta_0 \frac{\kappa - 1}{\delta} - 1 \geq 0,$$

which is equivalent to the condition

$$\tau \leq \tau_{max} \tag{A.1}$$

with

$$\tau_{max} = -\frac{1}{\gamma} \ln \left[\frac{1}{2} \left(\frac{\delta}{\beta_0} + 1 \right) \right].$$

We obviously require that

$$0 < \frac{1}{2} \left(\frac{\delta}{\beta_0} + 1 \right) < 1,$$

which is equivalent to

$$\delta < \beta_0. \tag{A.2}$$

Since $\tau_{max} \leq \ln 2/\gamma$, we consider for the rest of this section that inequalities (A.1) and (A.2) hold.

Assuming these conditions hold, we explicitly compute B^τ. By the definition of β_* and computing $\beta'_*(x)$, we obtain

$$B^\tau = \beta_* + \beta'_* x_* = \beta_* - \beta_* \frac{n x_*^n}{1 + x_*^n} = \beta_0 \frac{1}{(1 + x_*^n)^2} [1 + (1 - n) x_*^n]. \tag{A.3}$$

Because the parameter τ is our reference, we write B^τ, where τ is implicitly given in β_* through κ. The sign of B^τ plays an important role in determining the local stability conditions. From (A.3), it is clear that the sign of B^τ depends on the sign of

$$1 + (1 - n) x_*^n, \tag{A.4}$$

with $n \in \mathbb{R}^+$.

1. If $n \in [0,1]$, then $B^\tau > 0$.
2. If $n > 1$, then $1 - n < 0$ and

$$1 + (1-n)x_*^n \geq 0 \quad \Leftrightarrow \quad \tau \geq \tau_n, \tag{A.5}$$

where

$$\tau_n = -\frac{1}{\gamma} \ln \left\{ \frac{1}{2} \left[\frac{\delta}{\beta_0} \left(1 + \frac{1}{n-1} \right) + 1 \right] \right\}.$$

Note that for $n > 1$ we need

$$1 < \frac{1}{2} \left[\frac{\delta}{\beta_0} \left(1 + \frac{1}{n-1} \right) + 1 \right] \text{ or } \frac{n}{n-1}\delta > \beta_0.$$

Then, from the direct application of the Hayes theorem [31], we obtain the result given in the different cases of section 3.2.

Appendix B. Proof of Proposition 4.1. In order to present a proof as clearly as possible, we solve (4.4) only for the case where the initial condition

$$\varphi(t) > 1 \text{ for } t \in [-\tau, 0]$$

(the case where $\varphi(t) < 1$ works exactly in the same way). And we consider the situation where the period will be the shortest. In other words, when the solution increases, the slope of the curve representing the solution will be the steepest. Because of the continuity of φ and the solution x, there exists $t_1 > 0$ such that $x(t)$ and $x(t-\tau)$ are > 1 for $t \in [0, t_1]$. The solution of (4.4) then satisfies

$$\frac{dx}{dt} = -\delta x \quad \text{for } t \in [0, t_1].$$

Thus, the first part of the solution for this initial function is given by $x(t) = \varphi(0)e^{-\delta t}$, and this will persist until a time t_1 defined implicitly by $x(t_1) = 1$, or

$$t_1 = \frac{\ln \varphi(0)}{\delta}.$$

In the next interval, defined by $t \in [t_1, t_1 + \tau]$, the dynamics are given by the solution of

$$\frac{dx}{dt} = -\alpha x.$$

The solution on this interval is given by $x(t) = e^{-\alpha(t-t_1)}$. This solution persists until a time $t_1 + \tau$ at which point $x(t_1 + \tau) = e^{-\alpha\tau}$.

Note that the value of $x(t_1 + \tau)$ is independent of the initial function $x_0(t)$. This is a consequence of the particular dynamics of 4.4 which destroys all memory of the solution behavior when $x, x_\tau \geq 1$.

The solution in the next interval will be such that $x, x_\tau < 1$. Because we assume that Γ is sufficiently greater than α from Condition 4.6, the solution increases and there exists a

time t_2 such that $x(t_2) = 1$ with $t_2 \in [t_1 + \tau, t_1 + 2\tau]$. We note that this case corresponds to the situation where the period is the shortest. The other cases where $t_2 > t_1 + 2\tau$ can be computed with the same method and are not shown here.

It is clear that for $t_1 + \tau < t$, we need to set the condition $\Gamma > \alpha e^{-\alpha\tau}$ in order to get $\Gamma x_\tau > \alpha x$. Then, in a similar way, if we want the condition $0 < t_2 - (t_1 + \tau) < \tau$ to hold, it is easy to prove that we also need $\Gamma > (e^{\alpha\tau} - e^{-\alpha\tau})/\tau$. Since the condition (4.6) holds, then $0 < t_2 - (t_1 + \tau) < \tau$. On the interval $[t_1 + \tau, t_2]$, $x(t)$ is the solution of

$$\frac{dx}{dt} = -\alpha x + \Gamma x_\tau,$$

with $x_\tau(t)$ given by $x_\tau(t) = x(t - \tau) = e^{-\alpha(t-(t_1+\tau))}$. On this interval, $x(t)$ has the explicit form $x(t) = f_1(t)$, where

$$f_1(t) = e^{-\alpha(t-(t_1+\tau))}\left[e^{-\alpha\tau} + \Gamma(t - (t_1 + \tau))\right]. \tag{B.1}$$

The solution continues until the time t_2 defined by $x(t_2) = 1$.

On the next interval $[t_2, t_1 + 2\tau]$, we have $t - \tau \in [t_2 - \tau, t_1 + \tau] \subset [t_1, t_1 + \tau]$, so $x_\tau(t) = e^{-\alpha(t-(t_1+\tau))}$. Thus, the solution satisfies

$$\frac{dx}{dt} = -\delta x + \Gamma x_\tau \tag{B.2}$$

and is given by $x(t) = e^{-\delta(t-t_2)}[1 - \frac{\Gamma}{\beta_0}e^{\alpha(t_1+\tau)-\delta t_2}(e^{-\beta_0 t} - e^{-\beta_0 t_2})]$. On the next interval $[t_1 + 2\tau, t_2 + \tau]$, $x_\tau(t) = f_1(t - \tau)$. On this interval, the solution $x(t)$ also satisfies (B.2). It is given by

$$x(t) = e^{-\delta(t-(t_1+2\tau))}\left[x(t_1 + 2\tau) + \Gamma(j(t) - j(t_1 + 2\tau))\right],$$

where

$$j(t) = \frac{1}{\delta - \alpha}\left(e^{-\alpha\tau} + \Gamma(t - (t_1 + 2\tau)) - \frac{\Gamma}{\delta - \alpha}\right)e^{(\delta-\alpha)(t-(t_1+2\tau))}.$$

Then the maximum is given at a time $t_2 + \tau$ by

$$x(t_2 + \tau) = e^{-\delta(t_2-(t_1+\tau))}\left[x(t_1 + 2\tau) + \Gamma(j(t_2 + \tau) - j(t_1 + 2\tau))\right]. \tag{B.3}$$

After the time $t_2 + \tau$, both x_τ and x are greater than 1, and then the solution satisfies $x'(t) = -\delta x(t)$ until a time t_3, where $x(t_3) = 1$. We do not need to know x_τ. Consequently, on the interval $[t_2 + \tau, t_3]$, the solution is $x(t) = x(t_2+\tau)e^{-\delta(t-(t_2+\tau))}$, where $x(t_2+\tau)$ is given by (B.3). The time t_3 is then found to be

$$t_3 = \frac{\ln\left(x(t_2 + \tau)\right)}{\delta} + t_2 + \tau.$$

On the interval $[t_3, t_3 + \tau]$, the solution satisfies

$$\frac{dx(t)}{dt} = -\alpha x(t)$$

and is $x(t) = e^{-\alpha(t-t_3)}$. Then $x(t_3+\tau) = e^{-\alpha\tau} = x(t_1+\tau)$. It is then easy to see that we have established the existence of a limit cycle in our system with a period T given by $T = t_3 - t_1 \geq 2\tau$. The amplitude is the distance between the minimum reached for the first time at $t = t_1 + \tau$ with the value $x(t_1+\tau) = e^{-\alpha\tau}$, and the maximum reached for the second time at $t = t_2 + \tau$ given by (B.3) for the case where $\tau < t_2 - (t_1+\tau) < 2\tau$.

REFERENCES

[1] M. Adimy and L. Pujo-Menjouet, *A singular transport model describing cellular division.*, C. R. Acad. Sci. Paris Sér I. Math., 332 (2001), pp. 1071–1076.

[2] M. Adimy and L. Pujo-Menjouet, *Asymptotic behavior of a singular transport equation modelling cell division*, Discrete Contin. Dyn. Syst. Ser. B, 3 (2003), pp. 439–456.

[3] U. an der Heiden, M. C. Mackey, and H. O. Walther, *Complex oscillations in a simple deterministic neuronal network*, in Mathematical Aspects of Physiology, F. Hoppensteadt, ed., AMS, Providence, RI, 1981, pp. 355–360.

[4] U. an der Heiden and H. O. Walther, *Existence and chaos in control systems with delayed feedback*, J. Differential Equations, 47 (1983), pp. 273–297.

[5] J. Bélair, M. C. Mackey, and J. M. Mahaffy, *Age-structured and two-delay models for erythropoiesis*, Math. Biosci., 128 (1995), pp. 317–346.

[6] E. Beretta and Y. Kuang, *Geometric stability switch criteria in delay differential systems with delay dependent parameters*, SIAM J. Math. Anal., 33 (2002), pp. 1144–1165.

[7] S. Bernard, J. Bélair, and M. C. Mackey, *Sufficient conditions for stability of linear differential equations with distributed delay*, Discrete Contin. Dyn. Syst. Ser. B, 1 (2001), pp. 233–256.

[8] S. Bernard, J. Bélair, and M. C. Mackey, *Oscillations in cyclical neutropenia: New evidence based on mathematical modeling*, J. Theoret. Biol., 223 (2003), pp. 283–298.

[9] S. Bernard, J. Bélair, and M. C. Mackey, *Bifurcations in a white blood cell production model*, C. R. Biologies, 327 (2004), pp. 201–210.

[10] S. Bernard, B. Čajavec, L. Pujo-Menjouet, M. C. Mackey, and H. Herzel, *Modeling transcriptional feedback loops: The role of Gro/TLE1 in Hes1 oscillations*, Proc. Roy. Soc., submitted.

[11] H. Bolouri and E. H. Davidson, *Transcriptional regulatory cascades in development: Initial rates, not steady state, determine network kinetics*, Proc. Natl. Acad. Sci. USA, 100 (2003), pp. 9371–9376.

[12] A.-M. Buckle, R. Mottram, A. Pierce, G. S. Lucas, N. Russel, J. A. Miyan, and A. D. Whetton, *The effects of Bcr-Abl protein tyrosine kinase on maturation and proliferation of primitive haemotopoietic cells*, Molecular Medicine, 6 (2000), pp. 892–902.

[13] W. S. Bullough, *Mitotic control in adult mammalian tissues*, Biol. Rev., 50 (1975), pp. 99–127.

[14] F. Burns and I. Tannock, *On the existence of a G_0 phase in the cell cycle*, Cell Tissue Kinet., 3 (1970), pp. 321–334.

[15] R. Crabb, M. C. Mackey, and A. Rey, *Propagating fronts, chaos and multistability in a cell replication model*, Chaos, 3 (1996), pp. 477–492.

[16] G. Daley, R. Vanetten, and D. Baltimore, *Induction of chronic myelogenous leukemia in mice by the p210 bcr-abl gene of the Philadelphia-chromosome*, Science, 247 (1990), pp. 824–830.

[17] J. Dyson, R. Villella-Bressan, and G. F. Webb, *A singular transport equation modelling a proliferating maturity structured cell population*, Canad. Appl. Math. Quart., 4 (1996), pp. 65–95.

[18] J. Dyson, R. Villella-Bressan, and G. F. Webb, *Hypercyclicity of solutions of a transport equation with delays*, Nonlinear Anal., 29 (1997), pp. 1343–1351.

[19] J. Dyson, R. Villella-Bressan, and G. F. Webb, *An age and maturity structured model of cell population dynamics*, in Mathematical Models in Medical and Health Science, G. W. M. Horn and G. Simonnett, eds., Vanderbilt University Press, Nashville, TN, 1998, pp. 99–116.

[20] J. Dyson, R. Villella-Bressan, and G. F. Webb, *A nonlinear age and maturity structured model of population dynamics.* I. *Basic theory*, J. Math. Anal. Appl., 242 (2000), pp. 93–104.

[21] J. Dyson, R. Villella-Bressan, and G. F. Webb, *A nonlinear age and maturity structured model of population dynamics.* II. *Chaos*, J. Math. Anal. Appl., 242 (2000), pp. 255–270.

[22] J. Dyson, R. Villella-Bressan, and G. F. Webb, *A singular transport equation with delays*, Int. J. Math. Math. Sci., 32 (2003), pp. 2011–2026.
[23] C. J. Eaves and A. C. Eaves, *Stem cell kinetics*, Baillieres Clinical Haematology, 10 (1997), pp. 233–257.
[24] A. Elefanty, I. Hariharan, and S. Cory, *Bcr-Abl, the hallmark of chronic myeloid-leukemia in man, induces multiple hematopoietic neoplasms in mice*, EMBO J., 9 (1990), pp. 1069–1078.
[25] J. J. Ferrell, *Tripping the switch fantastic: How protein kinase cascade convert graded into switch-like outputs*, TIBS, 21 (1996), pp. 460–466.
[26] P. Fortin and M. C. Mackey, *Periodic chronic myelogenous leukemia: Spectral analysis of blood cell counts and etiological implications*, Brit. J. Haematol., 104 (1999), pp. 336–345.
[27] A. C. Fowler and M. C. Mackey, *Relaxation oscillations in a class of delay differential equations*, SIAM J. Appl. Math., 63 (2002), pp. 299–323.
[28] M. Gishizky, J. Johnsonwhite, and O. Witte, *Efficient transplantation of bcr-abl-induced chronic myelogenous leukemia-like syndrome in mice*, Proc. Natl. Acad. Sci. USA, 90 (1993), pp. 3755–3759.
[29] T. Haferlach, M. Winkemann, C. Nickenig, M. Meeder, L. Rammpetersen, R. Schoch, M. Nickelsen, K. Webermatthiesen, B. Schlegelberger, C. Schoch, W. Gassman, and H. Loffler, *Which compartments are involved in Philadelphia-chromosome positive chronic myeloid leukaemia? An answer at the single cell level by combining May-Grunwald-Giemsa staining and fluorescence in situ hybridization techniques*, Brit. J. Haematol., 97 (1997), pp. 99–106.
[30] C. Haurie, D. C. Dale, and M. C. Mackey, *Cyclical neutropenia and other periodic hematological diseases: A review of mechanisms and mathematical models*, Blood, 92 (1998), pp. 2629–2640.
[31] N. D. Hayes, *Roots of the transcendental equation associated with a certain difference-differential equation*, J. London Math. Soc., 25 (1950), pp. 226–232.
[32] T. Hearn, C. Haurie, and M. C. Mackey, *Cyclical neutropenia and the peripheral control of white blood cell production*, J. Theoret. Biol., 192 (1998), pp. 167–181.
[33] K. H. Howard, *Size and Maturity Structured Models of Cell Population Dynamics Exhibiting Chaotic Behavior*, Ph.D. thesis, Vanderbilt University, Nashville, TN, 2000.
[34] Y. Iizuka, A. Horikoshi, S. Sekiya, U. Sawada, T. Ohshima, and I. Amaki, *Periodic fluctuation of leukocytes, platelets and reticulocytes in a case of chronic myelocytic leukemia: The relation between leukocyte counts, CFU-C colony formation, CSA and CIA*, Acta Haematologica Japanica, 47 (1984), pp. 71–79.
[35] X. Jiang, C. J. Eaves, and A. C. Eaves, *IL-3 and G-CSF gene expression in primitive PH+CD*34(+) *cells from patients with chronic myeloid leukemia (CML)*, Blood, 90 (1997), pp. 1745–1745.
[36] M. Kelliher, J. Mcloughlin, O. Witte, and N. Rosenberg, *Induction of a chronic myelogenous leukemia-like syndrome in mice with v-Abl and Bcr-Abl*, Proc. Natl. Acad. Sci. USA, 87 (1990), pp. 6649–6653.
[37] J. Kevorkian and J. D. Cole, *Perturbation Methods in Applied Mathematics*, Springer-Verlag, Berlin, 1981.
[38] L. Kold-Andersen and M. C. Mackey, *Resonance in periodic chemotheray: A case study of acute myelogenous leukemia*, J. Theoret. Biol., 209 (2001), pp. 113–130.
[39] J. Konopka, S. Watanabe, and O. Witte, *An alteration of the human c-Abl protein in K*562 *leukemia-cells unmasks associated tyrosine kinase-activity*, Cell, 37 (1984), pp. 1035–1042.
[40] L. G. Lajtha, *On DNA labeling in the study of the dynamics of bone marrow cell populations*, in The Kinetics of Cellular Proliferation, F. Stohlman, Jr., ed., Grune & Stratton, New York, 1959, pp. 173–182.
[41] A. Lasota, M. C. Mackey, and M. Wazewska-Czyzewska, *Minimizing therapeutically induced anemia*, J. Math. Biol., 13 (1981), pp. 149–158.
[42] I. Lewis, L. Mcdiarmid, L. Samuel, L. To, and T. Hugues, *Establishment of a reproducible model of chronic-phase chronic myelogenous leukemia in NOD/SCID mice using blood-derived mononuclear or CD*34(+) *cells*, Blood, 91 (1998), pp. 630–640.
[43] T. Lugo, A. Pendergast, A. Muller, and O. Witte, *Tyrosine kinase-activity and transformation potency of Bcr-Abl oncogene products*, Science, 247 (1990), pp. 1079–1082.
[44] M. C. Mackey, *Unified hypothesis of the origin of aplastic anemia and periodic hematopoiesis*, Blood, 51 (1978), pp. 941–956.

[45] M. C. Mackey, *Dynamic haematological disorders of stem cell origin*, in Biophysical and Biochemical Information Transfer in Recognition, J. G. Vassileva-Popova and E. V. Jensen, eds., Plenum Publishing, New York, 1979, pp. 373–409.
[46] M. C. Mackey, *Periodic auto-immune hemolytic anemia: An induced dynamical disease*, Bull. Math. Biol., 41 (1979), pp. 829–834.
[47] M. C. Mackey, *Mathematical models of hematopoietic cell replication and control*, in The Art of Mathematical Modeling: Case Studies in Ecology, Physiology and Biofluids, Prentice–Hall, Upper Saddle River, NJ, 1997, pp. 149–178.
[48] M. C. Mackey, *Cell kinetic status of hematopoietic stem cells*, Cell Prolif., 34 (2001), pp. 71–83.
[49] M. C. Mackey and U. an der Heiden, *The dynamics of production and destruction: Analytic insight into complex behavior*, J. Math. Biol., 16 (1982), pp. 75–101.
[50] M. C. Mackey and P. Dörmer, *Continuous maturation of proliferating erythroid precursors*, Cell Tissue Kinet., 15 (1982), pp. 381–392.
[51] M. C. Mackey and R. Rudnicki, *Global stability in a delayed partial differential equation describing cellular replication*, J. Math. Biol., 33 (1994), pp. 89–109.
[52] M. C. Mackey and R. Rudnicki, *A new criterion for the global stability of simultaneous cell replication and maturation processes*, J. Math. Biol., 38 (1999), pp. 195–219.
[53] H. Moore and N. K. Lib, *A mathematical model for chronic myelogenous leukemia (cml) and t cell interaction*, J. Theoret. Biol., 227 (2004), pp. 513–523.
[54] H. G. Othmer, F. R. Adler, M. A. Lewis, and J. C. Dalton, eds., *The Art of Mathematical Modeling: Case Studies in Ecology, Physiology and Biofluids*, Prentice–Hall, Upper Saddle River, NJ, 1997.
[55] H. Peters, *Comportment chaotique d'une équation retardée*, C. R. Acad. Sci. Paris Sér I. Math., 290 (1980), pp. 1119–1122.
[56] L. Pujo-Menjouet, *Contribution à l'étude d'une équation de transport à retards décrivant une dynamique de population cellulaire*, Ph.D. thesis, Université de Pau et des Pays de l'Adour, Pau, France, 2001.
[57] L. Pujo-Menjouet and M. C. Mackey, *Contribution to the study of periodic chronic myelogenous leukemia*, Comptes Rendus de l'Académie des Sciences Paris Biologie, 327 (2004), pp. 235–244.
[58] S. I. Rubinow and J. L. Lebowitz, *A mathematical model of neutrophil production and control in normal man*, J. Math. Biol., 1 (1975), pp. 187–225.
[59] M. Santillan, J. Bélair, J. M. Mahaffy, and M. C. Mackey, *Regulation of platelet production: The normal response to perturbation and cyclical platelet disease*, J. Theoret. Biol., 206 (2000), pp. 585–903.
[60] L. F. Shampine and S. Thompson, *Solving DDEs*, Appl. Numer. Math., 37 (2001), pp. 441–445.
[61] J. A. Smith and L. Martin, *Do cells cycle?*, Proc. Natl. Acad. Sci. USA, 70 (1973), pp. 1263–1267.
[62] J. Swinburne and M. C. Mackey, *Cyclical thrombocytopenia: Characterization by spectral analysis and a review*, J. Theoret. Med., 2 (2000), pp. 81–91.
[63] N. Takahashi, I. Miura, K. Saitoh, and A. B. Miura, *Lineage involvment of stem cells bearing the Philadelphia chromosome in chronic myeloid leukemia in the chronic phase as shown by a combination of fluorescence-activated cell sorting and fluorescence in situ hybridization*, Blood, 92 (1998), pp. 4758–4763.
[64] H. O. Walther, *Homoclinic solution and chaos in* $\dot{x}(t) = -\mu x(t) + f(x(t-1))$, Nonlinear Anal., 5 (1981), pp. 775–788.
[65] G. F. Webb, *Theory of Nonlinear Age-Dependent Population Dynamics*, Monogr. Textbooks Pure Appl. Math. 89, Dekker, New York, 1985.
[66] X. W. Zhang and R. B. Ren, *Bcr-Abl efficiently induces a myeloproliferative disease and production of excess interleukin-3 and granulocyte-macrophage colony-stimulating factor in mice: A novel model for chronic myelogenous leukemia*, Blood, 92 (1998), pp. 3829–3840.